PROTO-SPHERA confines axisymmetric plasma tori in absence of any toroidal magnet and just in presence of a static poloidal magnetic field

FSN Department, CR-ENEA *Frascati*

Franco Alladio, Paolo Micozzi, Fabrizio Andreoli, Gerarda Apruzzese, Luca Boncagni, Paolo Buratti, Fabio Crescenzi, Ocleto D'Arcangelo, Giuseppe Galatola Teka, Edmondo Giovannozzi, Andrea Luigi Grosso, Matteo Iafrati, Alessandro Lampasi, Violeta Lazic, Simone Magagnino, Valerio Piergotti, Mario Pillon, Selanna Roccella, Giuliano Rocchi, Alessandro Sibio, Benedetto Tilia, Onofrio Tudisco, Alessandro Mancuso[retired] , Vincenzo Zanza[retired]

FSN Department, CR-ENEA *Frascati and* CREATE *Consortium*

Giuseppe Maffia, Brunello Tirozzi,

PlasmaTech Spin-off of Pisa University

Francesco Giammanco, Paolo Marsili

Pisa University

Danilo Giulietti

Nature Physics (2018)

Abstract

The PROTO-SPHERA experiment, using DC helicity injection driven by a voltage applied between electrodes, has formed and sustained up to ½ sec magnetically confined current carrying tori in presence of a pre-existing axisymmetric configuration of magnetostatic poloidal field only and in absence of any doubly connected toroidal magnet. This result provides the first hints that future Fusion machines could be built with permanent magnets only.

The relevance of a magnetic confinement machine built by axisymmetric permanent magnets only

The use of permanent magnets in toroidal plasma confinement would be paramount for simplifying the design and the complexity of a Controlled Fusion rector based upon magnetic confinement. It would remove any direct dissipation connected with currents flowing inside the magnetic field coils and would even have great advantages with respect to superconducting coils, which share with permanent magnets the absence of ohmic dissipation but require a sophisticated cryogenic system; such a system entails a number of other thermal dissipations, in order to maintain the superconducting coils at the required low temperature conditions. One of the appealing features of future axisymmetric magnetic confinement thermonuclear reactors is that, if they will also contain open field lines and will be endowed with two degenerate X-points (null or neutral magnetic field points) at their opposite edges on the symmetry axis[1], they could even become Fusion space thrusters, able to propel Nuclear Fusion rockets in space, through the preferential expulsion of charged Fusion products from one of the two degenerate X-points[2], which will act as a "plasma nozzle". In the deep space environment the use of permanent magnets for a Fusion space thruster is the most reasonable possibility, as superconducting magnets would imply the maintenance and the servicing of a reliable large scale cryogenic system, an endeavor that would be very impractical to implement, if not outright impossible.

The use of permanent magnets in toroidal plasma confinement has never been considered so far. The reasons were mainly two: a) the necessity in the case of axisymmetric toroidal pinches configuration (such as Tokamaks[3], RFPs[4], etc…) of creating and of sustaining the plasma with the help of variable currents in a number of magnetic field coils, i.e. central transformer coils wound in a variety of positions around the main axis of the torus for breaking-down inductively the plasma and for achieving and sustaining the required toroidal current inside it; furthermore vertical field coils with variable currents, able to counteract changes of the equilibrium position, must be present, in particular as abrupt plasma displacements can trigger MHD instabilities that can result in the final disappearance of the plasma torus (disruptions, in particular those called "vertical displacement events"[5]). The need expressed in point a) could be overcome in the case of non-axisymmetric configurations[6] (such as Stellarators, Torsatrons, etc…) where in principle no variable field is needed. However the other main reason against permanent magnets is even more compelling and cannot be avoided even by Stellarators: b) a toroidal field magnet (irrespective of its more ore less perfect axisymmetry or the plain absence of axisymmetry) cannot be built with permanent magnets only, the reason being that the single-valued magnetic scalar potential that describes any magnetostatic field outside permanent magnets would be many-valued in the doubly connected domain of a toroidal field magnet, this simple fact implies the necessity of a net poloidal current through the torus hole.

This apparently established picture could be completely changed by the results recently obtained in the PROTO-SPHERA experiment[7], where a confined plasma torus carrying a net toroidal current has been formed and maintained in absence of any kind of toroidal magnet and in a pre-existing axisymmetric configuration of static poloidal field, which fills a simply connected region containing the whole plasma; in such simply connected region the static field can be derived from a pure single-valued magnetic scalar potential. This overall plasma configuration is furthermore not susceptible to disruption phenomena and the correct value and shape of the pre-imposed poloidal magnetic field determines the toroidal plasma current that can flow inside the torus: if the shape of the magnetostatic field is the correct one, an almost axisymmetric torus forms immediately after the breakdown of the plasma; if the shape of the poloidal field is slightly incorrect the torus forms from an initial "quasi-axisymmetric cusp" plasma configuration, which appears with relevant non-axisymmetric components and then relaxes into the almost axisymmetric torus; if the shape of the pre-imposed poloidal magnetic field is more incorrect multiple tori and lop-sided tori can be formed and sustained, always in presence of large non axisymmetric components.

The results found in PROTO-SPHERA with an axisymmetric static field configuration in a simply-connected domain have been produced up to now by normal conducting poloidal field (PF) coils only, so this paper does not yet deal with a redesign of PROTO-SPHERA in terms of equivalent axisymmetric permanent magnets, which remains to be addressed in future. A number of engineering issues engendered by a magnetic confinement Fusion machine built with permanent magnets have still to be evaluated, such as: risks of permanent magnets demagnetization, due to the presence of toroidal and poloidal currents inside the plasma (which will remains the only part of the overall configuration where the magnetic field is rotational); the maximum feasible value of the magnetic field strength with present and with foreseeable permanent magnet technology, as a function of the dimensions of the apparatus; and finally the mechanical limits introduced by the strength of the interactions among the permanent magnets.

Present status of PROTO-SPHERA in Phase-1 and additions for Phase-2

The PROTO-SPHERA experiment was recently built in its Phase-1 version[8,9] in the ENEA-Frascati Reserch Center (Fig.1a). Its final purpose is to form a

Spherical Torus (ST, with closed flux surfaces) not around a metal centerpost, as in the case of conventional and of spherical Tokamaks, but around a Plasma Centerpost (PC, with open flux surfaces and fed by annular electrodes), which is an arc discharge with the magnetic structure of an axisymmetric linear screw pinch, i.e. a pinch which has both an azimuthal (toroidal) as well as a longitudinal (poloidal) B field component.

Fig.1: The general layout of the experiment.

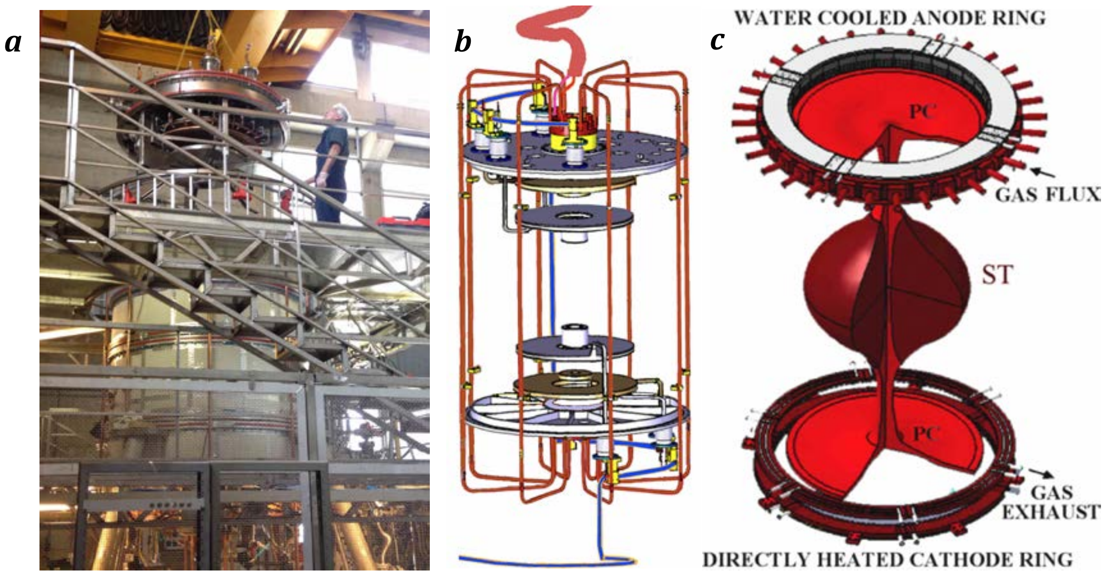

a, The PROTO-SPHERA load assembly in Frascati, while the annular anode is being inserted (year 2015). b, The copper bars (shown in red) ouside the vacuum vessel, that return the Centerpost plasma current from a lower collecting ring to an upper outer coaxial ring, are the equivalent of the outer part of a toroidal magnet in a Tokamak; the coaxial cable that feeds the Phase-1 PF coils is shown in blue. c, Scheme of Spherical Torus around the Plasma Centerpost and annular electodes

The original idea was that of getting rid of all the metal components (toroidal field coils and ohmic transformer) at the center of the plasma configuration, which are the most critical component of a Spherical Tokamak design. Thin copper bars outside the vacuum vessel, that return the Centerpost plasma current from a lower collecting ring to an external upper ring, are the only components reminiscent of the outer part of a toroidal magnet in a Tokamak (Fig. 1b).

Therefore the PROTO-SPHERA system is a simply connected configuration: in the final Phase-2 version it will be composed by a Spherical Torus (with equatorial plane diameter $2R_{sph}$=0.7 m and a toroidal plasma current $I_{ST}\leq 240$ kA) and by an arc discharge with length $L_{Pinch}\approx 2$ m and midplane diameter ≈0.08 m, fed by annular electrodes (with radius = 0.40 m and height=0.04 m), with open flux surfaces and a Plasma Centerpost current (or electrode plasma current) equal to I_e=60 kA. The Plasma Centerpost takes the shape of a mushroom in front of both annular electrodes (Fig.1c).

However, in order to clarify the breakdown conditions and the Plasma Centerpost stability before the formation of the Spherical Torus, the Phase-1 version of the experiment was designed as a reduced setup of the final PROTO-SPHERA machine and was devoted to assess and clarify the most critical points of the PROTO-SPHERA configuration from the PC point of view: Fig. 2a shows the overall apparence of the Phase-1 plasma discharge, by superposing the images of 4 different cameras (with some arbitrariness, as they do not look at the same azimuthal angle around the machine), the cathode slow camera on the bottom, then the fast camera in the main chamber, the two anode slow cameras on the top, tilted at two different angles to be able to show both the anodic plasma as well as the “plasma nozzle”[2] from the upper degenerate X-point. PROTO-SPHERA in Phase-1 has explored the starting phase of the PROTO-SPHERA discharge, in presence of internal poloidal field (PF) shaping coils alone, see Fig. 2b: Group-B PFInt coils, all connected in series among themselves and fed by a unique power supply, and therefore in absence of the Spherical Torus. The load assembly was built in the years 2007-2009 by ASG Superconductors in Genova (Italy) inside the 2 m diameter START[10] vacuum vessel, kindly gifted by the Euratom-UKAEA British Association.

Fig.2: Phase-1 and Phase-2 of PROTO-SPHERA.

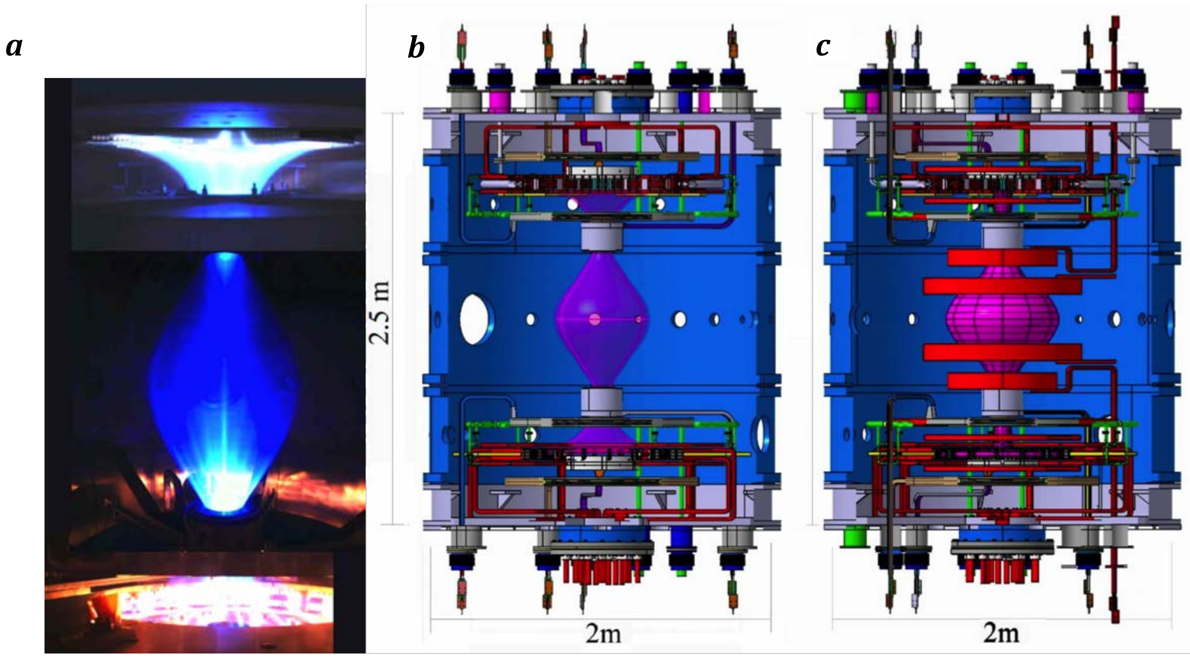

a, PROTO-SPHERA Ar Plasma Centerpost discharge: pictures from 4 cameras (at different azimuthal angles) are superposed, the plasma goes through the upper and lower PF2 coils. b, Inside view of the Phase-1 load assembly. c, Inside view of the Phase-2 load assembly, both showing all components internal to the vacuum vessel. Anode is on top and its feed-throughs are on the top lid, cathode is on bottom and its feed-throughs are on the bottom lid. All PFInt coils are fed from the lid which is most near to each of them.

To complete the machine other 10 poloidal field compressing coils will be built (Fig. 2c), the 4 largest among them being in charge of providing the vertical field required by the ultra-low aspect ratio torus of Phase-2, the other 6 coils being just correcting and focalizing coils, in charge of maintaining the correct position of both the mushroom-shaped lower and upper Plasma Centerpost with respect to both annular electrodes.

Fig.3: The cathode of PROTO-SPHERA.

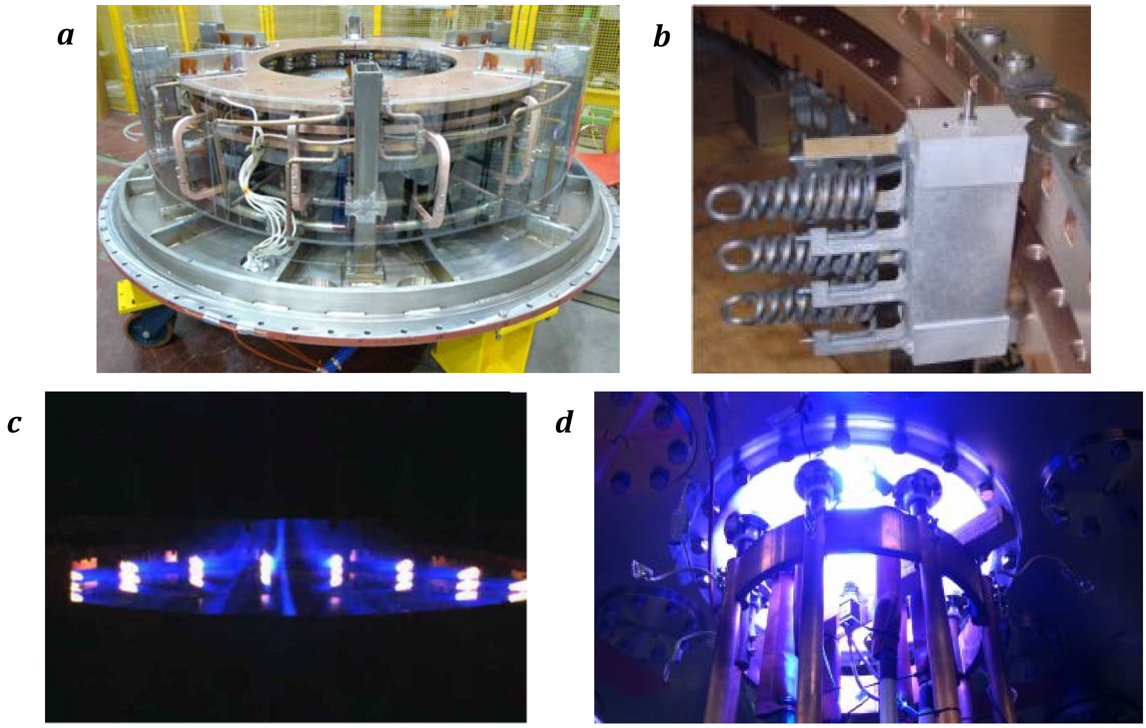

a, The annular cathode resting on the bottom lid. b, Module of 3 Tungsten filaments inserted into the Copper body of the cathode. c, Picture from the cathode camera for Ar shot #842: plasma filaments originate from each individual W filament heated to ~2900 °C. d, View of polycarbonate cathode lower bus-bar flange form below, while Ar plasma is present: the external copper ring collects the plasma electrode current I_e; inside the copper ring each of the six cables carries 1.7 kA, typically at 18 V rms, in order to heat the 9 W filaments present per phase.

Also these further 10 Group-A PFint (compression) coils will be connected in a second series among themselves and fed by a second unique power supply.

The Phase-1 cathode (Fig. 3a) is the final directly heated (Fig. 3b) PROTO-SPHERA cathode, but it is only partially filled (see Fig.3c) with doubly wound Tungsten VM (WVM) filament modules[11,7] (see Fig. 3b, each W filament reminds of a "Caduceus" of the winged god Mercury): 54 filaments of Phase-1 vs. the 324 filaments of Phase-2. So each filament was tested in Phase-1 while delivering the maximum plasma current (~185 A) envisaged for Phase-2.

The purpose of the doubly wound WVM filaments, apart from providing a source of electrons for breaking-down the plasma, is also to extend the surface of the plasma-metal interaction to an area much greater than the one which could be provided by a simple annular (ribbon-like) cathode-plasma interface.

The electrical power supply for heating up the cathode is a six-phased AC machine, built by EEI of Vicenza (Italy), able to deliver 1.7 kA up to 25 V rms to the 9 W filaments present per phase (Fig. 3d) at this moment; its current capability will be increased to 10 kA per phase in the Phase-2 version, to be able to heat to ~2900 °C the final 54 filaments present per phase.

The power supply for the 8 Group-B PFInt coils, built by EEI of Vicenza (Italy), is the final one: a DC machine that delivers 2 kA at 350 V DC to the series of the 8 coils .

The anode is also the final one[11,7]; it is a gas-puffed hollow annular anode whose plasma facing material is Copper-Tungsten (W-Cu, with 95% W); from its rear the gas discharge is puffed into many hundreds of front holes, opened towards the plasma, so that the plasma is on its part able to enter inside these holes: the purpose of them is to extend the surface of the plasma-metal interaction to an area much greater than the one which could be provided by a simple annular (ribbon-like) anode-plasma interface.

Fig.4: The anode of PROTO-SPHERA.

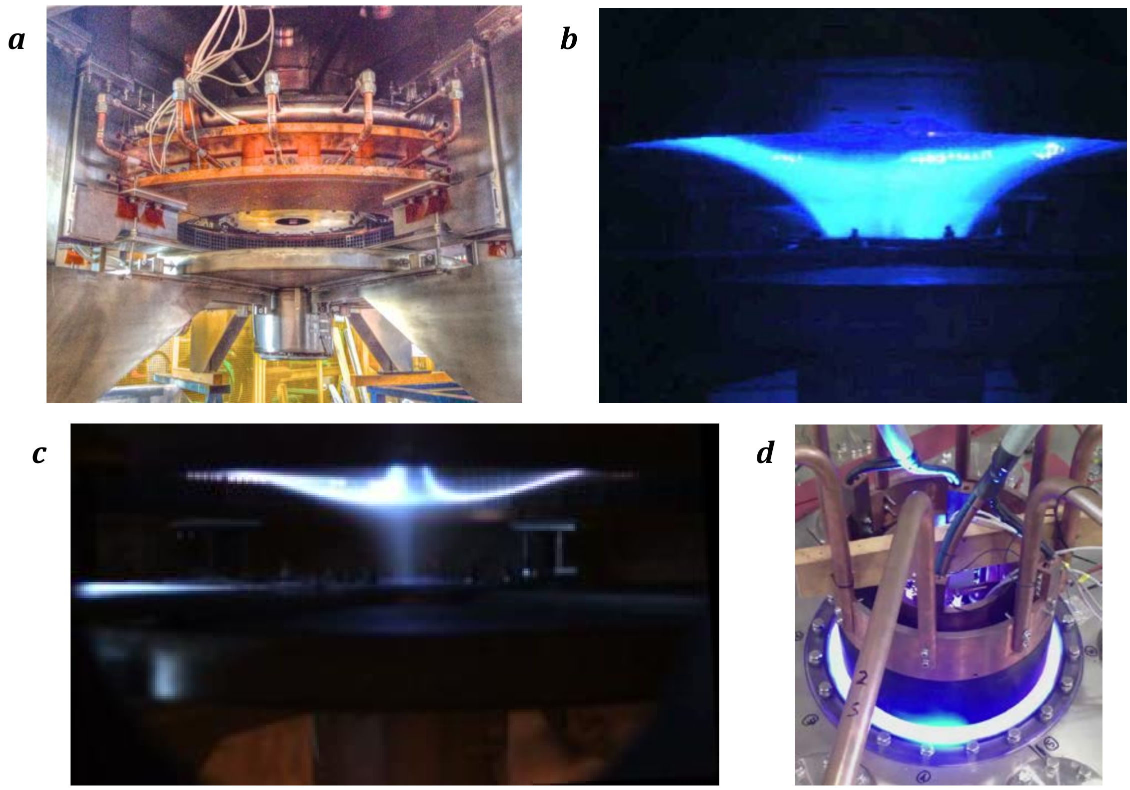

a, The annular cathode hanging from the top lid. b, Picture from the anode camera for Ar shot #954. c, View of the “plasma nozzle”[2] from the upper degenerate X-point on top of the annular anode, taken when the Plasma Centerpost is being switched off. d, View of polycarbonate anode upper bus-bar flange form above, while Ar plasma is present: the internal copper ring drives, through 6 feed-troughs, the electrode plasma current I_e to the anode, the external copper ring collects the same current I_e from 8 copper bars that connect to the lower ring of Fig. 3d.

The Plasma Centerpost power supply, built by EEI of Vicenza (Italy), is instead limited to the first unit (I_e =10 kA at 350 V DC); a second unit will be built in Phase-2, able to increase the electrode plasma current up to I_e=60 kA. A further power supply for the new Group-A PFInt compression coils will be built in Phase-2 as a DC machine able to deliver 1.2 kA at 600 V to the 10 new coils connected in series. With the exception of the six-phased AC Cathode heating power supply all the conductors that carry the currents of the power supply are coaxial cables (see Fig. 1b); in particular the Plasma Centerpost power supply is fed through two coaxial metal rings on top of the machine (Fig. 4d), in order to minimize any error field.

The Plasma Centerpost obtained in Phase-1

To obtain the Plasma Centerpost the procedure is to begin with heating the W filaments (about 30 sec before the plasma break-down); when the filaments have reached ~2900 °C the Group-B PFInt coils are energized, the shaping field (Fig.5a) is produced inside the 4 cm thick Aluminum vessel and immediately after (with about a few 10s ms delay) the Centerpost power supply is fired, the screw pinch plasma is produced and can be maintained at the full Phase-1 electrode plasma current I_e=10 kA for ~1 sec. Two gases were used for producing a plasma: Argon and Hydrogen. Argon clearly has no interest whatsoever for Controlled Fusion, it was employed only as its break-down voltage is very low and in the first 2 and 1/2 years of the machine operation (mid 2015 to end of 2017) Ar was the gas of choice for learning how to cure a number of insulation problems, that are here of not so great interest and that will be detailed in a paper devoted to this specific topic. The only point that has to be underlined here is that among other insulations a 2 mm thick polycarbonate foil lines the inside of the Aluminum vessel and two 1 cm thick polycarbonate diaphragms have been glued to this foil near the two PF2 "mirror coils" (Fig. 5a contains all the PF coils names): the translucent polycarbonate disturbes the images collected by a fast wide-angle videocamera looking at the Plasma Centerpost, because multiple reflections occur and are clearly seen in Fig. 5b, as in almost all other camera images shown in this paper. The 10 kA Plasma Centerpost in Ar (Fig. 5b) was obtained in January 2018, its break-down anode to cathode voltage was ~90 V, and the flat-top of the electrode plasma current was sustained while the DC voltage applied to electrodes increased to ~200 V. The diameter of the 10 kA Ar Plasma Centerpost on the equatorial plane was about $2R_{sph}$ =50 cm.

Initial attempts of measuring the Ar Plasma Centerpost equatorial line-averaged electron density $\langle n_e \rangle$ by a 4 mm interpherometer[12] were unsuccessful, because the density was higher than expected but they gave anyhow an interesting information: although the 4 mm microwave was in cutoff no reflected signal was observed, hinting to the existence of a significant gradient of electron density from bottom (larger) to top of the Centerpost (smaller), able to deflect the microwave beam in the vertical direction; also the visible images of Ar discharges (Fig. 2a and 5a) show a relevant vertcal inhomogeneity of the light emission.

Fig.5: The Plasma Centerpost obtained in Phase-1.

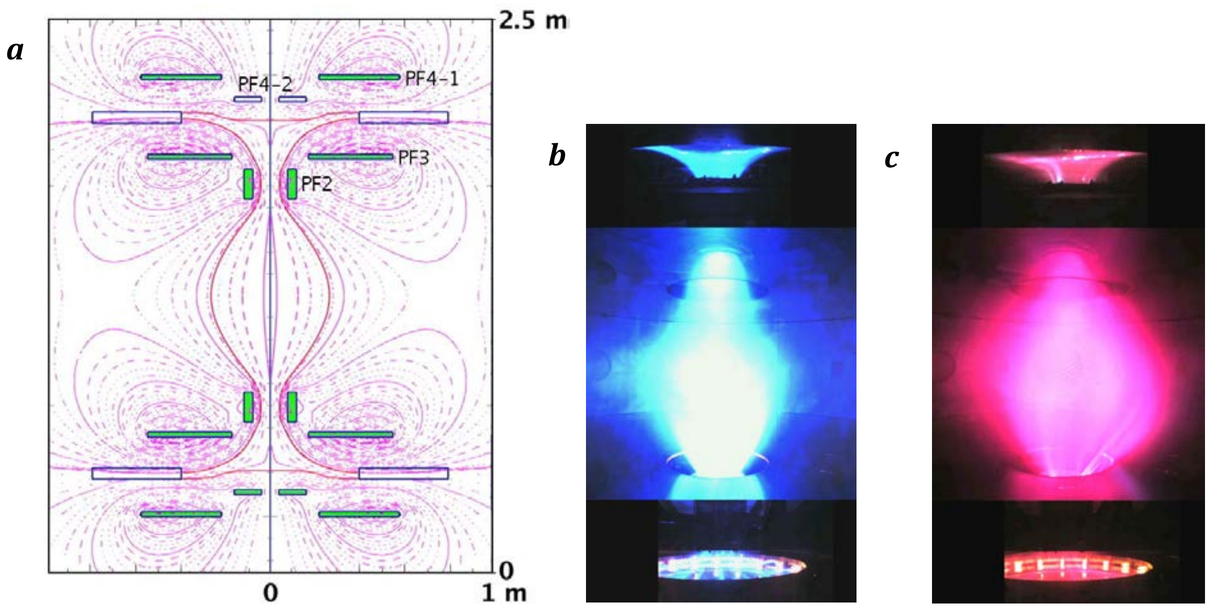

a, Shaping magnetic field produced by the 8 Group-B PFInt coils, the upper PFInt coils are denominated in this figures, the lower ones being mirror symmetric across the equatorial plane. b, Centerpost discharge #954 in Ar at I_e=8.5 kA: pictures from 3 cameras (at different azimuthal angles) are superposed. c, Centerpost discharge #969 in H at I_e =8.5 kA .

The line-averaged electron density $\langle n_e \rangle$ of the Ar Centerpost has been thereafter measured on the equatorial plane, by a common-path Second Harmonic Interferometer (SHI)[13,14]. The SHI, developed by the "Plasma Diagnostics & Technologies" (a spin-off of the University of Pisa), is a device insensitive-to-vibrations, which has allowed an easy installation on the machine, thanks to a compact modular design. The equatorial line-averaged electron density $\langle n_e \rangle$ of Ar Plasma Centerpost was found to exhibit a linear dependence upon the electrode plasma current: $\langle n_e \rangle \propto I_e$, with $\langle n_e \rangle = 4 \cdot 10^{20}$ m^{-3} at I_e =10 kA. As the magnetic field lines start from and end to electrodes the Plasma Centerpost temperature cannot be larger than a few eV: it has not yet been measured in the main chamber but it has been determined up to now only at the edge of the anodic mushroom-shaped plasma by a Langmuir probe: the local electron temperature at this point, just at the edge of the anode discharge, was measured to be from 2 to 8 eV, while in the same series of Langmuir probe measurements the local electron plasma density varied from $5 \cdot 10^{19}$ m^{-3} to $2 \cdot 10^{19}$ m^{-3}. Optical emission (OE) from the Proto-Sphera device is detected by a compact spectrometer array[15] covering the range 235-790 nm with the resolution from 0.09 nm in UV to 0.14 nm in IR. Preliminary results of spectroscopic observations from a line of sight along the plasma equator indicate that in Hydrogen discharges the visible spectrum shows only the Hydrogen lines, whereas the UV spectrum indicates limited amounts of metallic impurities.

Also Hydrogen has no interest whatsoever for Controlled Fusion[16], but it is indicative of the behavior of Deuterium that will be used in the Phase-2 of the experiment. The 10 kA Plasma Centerpost in H (Fig. 5c) was obtained also in January 2018, its break-down voltage was ~320 V and the flat-top of the electrode plasma current was sustained while the DC voltage applied to electrodes decreased to ~220 V. The diameter of the H Plasma Centerpost at 10 kA on the equatorial plane was about $2R_{sph}$ =60 cm. In Hydrogen discharges electrode plasma currents much lower than 10 kA exhibited large variation and were rather difficult to be maintained with steady currents, so the only reliable line-averaged electron density measurements were performed at I_e =10 kA, where the equatorial line-averaged electron density was $\langle n_e \rangle = 1.5 \cdot 10^{20}$ m^{-3}. Both Plasma Centerpost discharges (Ar and H) were sustained until the DC voltage was applied on the electrodes (1 sec). The much feared anode arc-anchoring of the plasma[17,18] (i.e. the possibility that the discharge in front of the annular anode could concentrate upon a restricted anode spot, inflicting local damage) never occurred; the explanation of the absence of anode arc-anchoring resides in the rotation of the Plasma Centerpost in the azimuthal (toroidal direction), which is evident in the largest central portion of the plasma from the visible light movies collected by a fast camera (see Fig. 5) with full image of 1024•1024 pixels and sampling rate of ~3kHz. The Plasma Centerpost, observed in visible light, rotates approximately at a frequency of ½ kHz both in Ar as well as in H plasmas. The cause of such a rotation appears to be the electrostatic charging of the PF coils casings by the plasma itself. As a matter of fact all the 8 Group-B PFInt coils present inside the vacuum vessel have a floating electric potential, also the top part of the vessel, composed by an AISI304 ferrule-and-lid (see Fig. 6a, which enumerates again the names of the PFInt coils) is at floating electric potential, as well as the lower symmetrical part of the vacuum vessel, both upper and lower parts are separated from the electrically grounded Aluminum cylinder by two 1 cm thick insulating Polycarbonate rings. The total height of the PROTO-SPHERA vacuum vessel is therefore extended (with respect to START, which was originally 2 m tall) by the two ferrules and reaches 2.52 m.

Fig.6b shows that, albeit the magnetic flux surfaces are up/down symmetric (even parity, see Fig.5a), the electrostatic potential is up/down asymmetric (does not have an odd parity), i.e. the plasma charges with a different pattern the PFInt coils on the anode and on the cathode side. It seems a reasonable guess to suppose that this asymmetry is connected to the vertical gradient of electron density along the Plasma Centerpost.

Fig.6: The electrostatic charging of the internal floating components

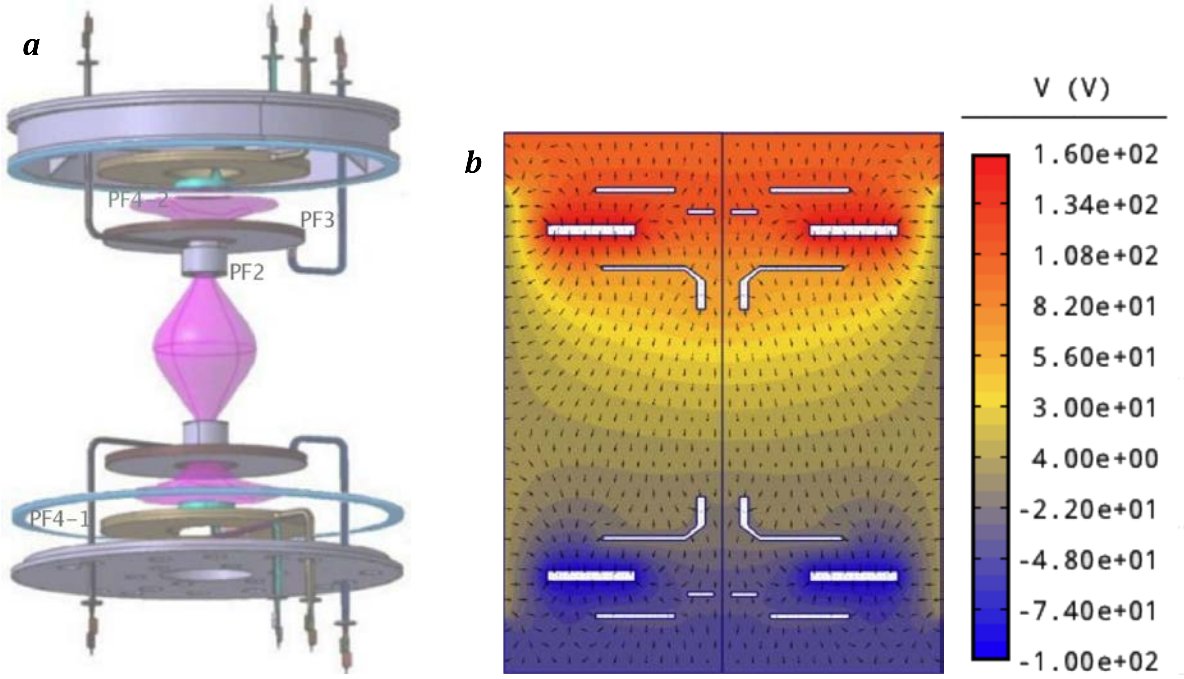

a, Inside view of the Phase-1 experiment: the Centerpost Plasma is drawn in pink colour; the Aluminum START cylindrical vessel, the lower AISI304 ferrule and the electrodes are removed: two polycarbonate insulators separate the Aluminum vessel from the two ferrules on top and bottom. b, The electrostatic potential in H discharges at I_e=10 kA (shown with different colors) is not up/down antisymmetric, i.e. the plasma charges the PFInt coils on the anode side with a different pattern of electric potential with respect to the cathode side.

In Hydrogen plasma at 10 kA, during the current flat top, the anode (top) is charged to +140 V while the catode (bottom) at -80 V, the top lid and ferrule are charged at +95 V while the bottom ferrule-an-lid are charged at -55 V, the PF4 coils ("plasma nozzle" coils near the null magnetic field point, see Fig. 1c) are charged to +50 V on top and to -10 V on bottom and the PF2\3 coils (mirror coils) are charged to +95 V on top and -40 V on bottom.

Therefore there is no up/down compensation in the E∧B drift of the plasma, that would be opposite in the anode and cathode region: the top anode region has the larger electrostatic field, therefore it dominates and determines the direction of the net plasma rotation. With the magnetic field due to the PFInt coils going upwards from cathode to anode and the electrostatic field going obviously downwards from anode to cathode, the net plasma rotation is clockwise, as seen from the top of the machine .

From Fig. 5a) it is possible to see that an ordinary X-point (poloidal field B_{pol}=0) is present on the equatorial plane inside the vacuum vessel at only ~30 cm from the Aluminum wall. In order to change the magnetic boundary conditions four external additional PFExt coils were added (Fig. 7a). However the presence of the 4 cm thick Aluminum vacuum vessel and of the two groups of AISI304 ferrule-and-lid on top and bottom (see Fig. 6a) introduces a skin current that opposes the applied external magnetic and that is totally dissipated in the Aluminum only after 0.6 sec. Therefore, in order to achieve steady state conditions with the combined (internal + external) shaping field, the break-down of the plasma must be delayed by ~0.6 sec: the maximum duration of the plasma discharge is then reduced from 1.1 sec to just 0.5 sec.

If the current flowing inside the two PFExt nearer to the equatorial plane is in the same direction as the current inside the PF2\PF3 coils the ordinary X-point is removed from inside the vacuum vessel (Fig.7b); in this case the current flowing in the two PFExt coils is in the same direction also with the plasma current winding in toroidal direction inside the Plasma Centerpost; therefore the vertical field introduced will have the wrong effect with respect to helding in equilibrium a possible plasma torus, should it form.

Fig.7: Destabilization of Plasma Centerpost by external vertical field coils

a *b* *c* *d*

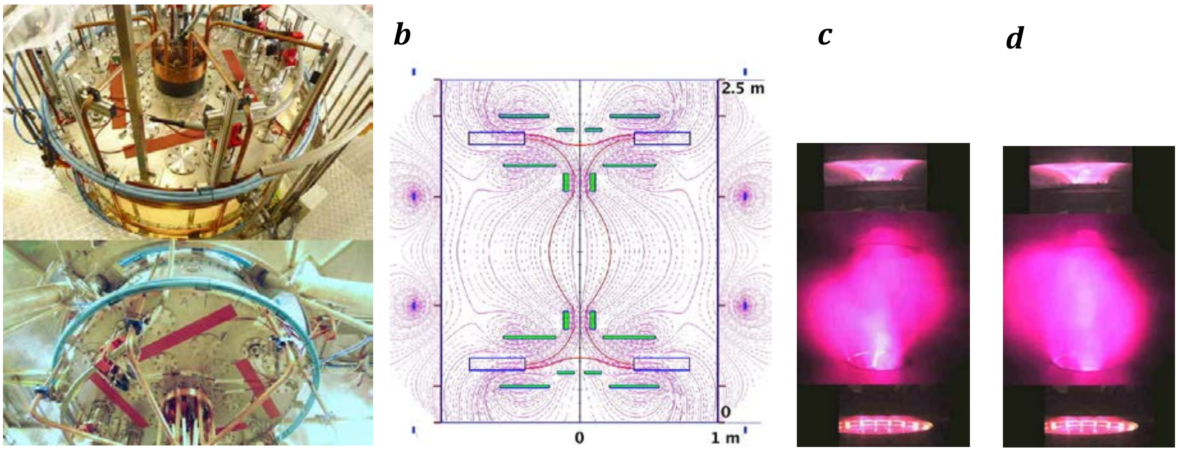

a,b, The four additional PFExt coils added outside the vessel (light blue color), viewed from the top and from the bottom lid. The upper copper coaxial ring structure is the entrance of the Centerpost power supply feed, shown in more detail in Fig. 4d. and the lower plasma current collecting copper ring is better shown in Fig. 3d. c, Shaping magnetic field produced by the 8 Group-B PFInt coils and PFExt coils for shot #985: the equatorial ordinary X-point, that in Fig.5d was inside the vacuum vessel, is displaced outside of it. d,e, Centerpost discharge #985 in H at I_e =10 kA, bulging differently at two distinct time slices: pictures from 3 cameras (at different azimuthal angles) are superposed.

Obviously the result is that the Plasma Centerpost becomes unstable and bulges helicoidally outwards (Fig. 7c and 7d). This happens when the rotational transform of the Plasma Centerpost (calculated from anode to cathode) overcomes the semi-integer value $\iota_e \geq 1/2 \, (q_e \leq 2$ in terms of the inversely defined safety factor), which corresponds to $I_e \geq 8.5$ kA .

The calculations of the shaping magnetic fields shown in Fig.5a and Fig. 7b confirm that on the symmetry axis PROTO-SPHERA a degenerate X-point (where B =0) is present (in correspondence of the observed plasma “nozzle” of Fig. 2a): this is the feature that could enable a Controlled Fusion ignited configuration similar to PROTO-SPHERA to become a Fusion space thruster, able to propel Nuclear Fusion rockets in space.

The Argon Tori obtained in Phase-1

The presumed way of producing a Plasma Spherical Torus in Phase-2 of the PROTO-SPHERA[7] experiment was to start with the Group-B PFInt (shaping coils) at the same value of current as in Phase-1, then to break-down the Plasma centerpost, driving it up to at I_e=8.5 kA, and thereafter to increase rapidly (~1 ms) both the Centerpost current I_e to 60 kA and, at about the same time, the current in the Group-A PFInt compression coils. Such a current increase of the compression coils would have produced an equilibrium vertical field able to contain the Torus and would have provided, at the same time, a part of its toroidal current by the inductive effect. This scenario gives the calculated Spherical Torus shown in Fig. 8a. Instead what was attempted in PROTO-SPHERA Phase-1 was just to impose inside the two external additional PFExt coils nearer to the equatorial plane a current flowing in the opposite toroidal direction with respect to the current flowing inside the PF2\PF3 coils and therefore also opposite to the plasma current winding in toroidal direction inside the Plasma Centerpost. Therefore the vertical field introduced had the right effect with respect to helding in equilibrium a possible plasma Torus, was it going to be formed. The first effect of the torus formation is that, because of the ouward force due to the closed toroidal plasma current, the Plasma Centerpost takes on the outboard of its equatorial region, an approximately spherical shape.

Fig.8: Plasma tori, what is foreseen for Phase-2 and obtainable in Phase-1

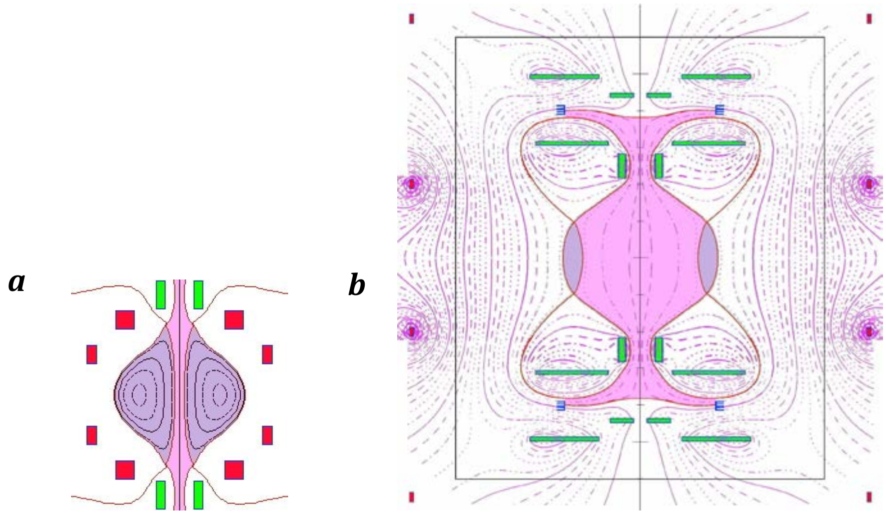

a, Spherical Torus calculated for the Phase-2 of the experiment, when nearby compression coils (drawn in red) will be added inside the vessel. b, Calculated equilibrium of a Torus carrying a toroidal current I_{ST} =7 kA, with the PFExt compression coils added in Phase-1 outside the vessel.

Of course the portion of closed flux surfaces carved out by the torus in Phase-1 from the spherical shape of the equatorial outboard region of the Plasma Centerpost would have been quite narrow. The field generated by the external additional PFExt coils in Phase-1 is just an almost vertical field (see Fig. 8b which shows a calculated equilibrium[19] for a Plasma Centerpost carrying an electrode current I_e=10 kA surrounded by a torus carrying a toroidal current I_{ST} =7 kA) and misses the shaping character of the future

Group-A PFInt coils of Phase-2, which have been designed in such a way as to carve from the spherical shape of the equatorial outboard region of the Plasma Centerpost the largest possible portion of closed flux surfaces (Fig. 8a).

The two other external additional PFExt coils (the ones farthest from the equatorial plane) are better fed with opposite direction of current with respect to the two PFExt nearer to the equatorial plane (see Fig. 8b), this choice helps in restoring, to some extent, the correct position of the two plasma mushrooms in front of both electrodes, that otherwise, because of the equilibrium changes due to the vertical field, would have been rather marginally wetted by the plasma.

All the four PFext coils were initially still fed in series with the Group-B PFInt coils, as the voltage deliverable by the PFInt power supply (2 kA at 350 V DC) was overabundant: even slightly larger than the additional voltage demanded by the PFext coils for producing the vertical field required by the Ar torus formation.

The calculated equilibrium configuration[19] of the Plasma Centerpost alone, in case the torus would have not been formed, was characterized by two ordinary X-point (poloidal field B_{pol}=0) present on the equatorial plane inside the vacuum vessel, at only ~32 cm from the symmetry axis (Fig. 9a), making in principle the Plasma Centerpost much narrower than in all previous cases. As a matter of fact when the electrode plasma current was limited to ~I_e =3 kA in Argon the plasma conformed to this narrow shape (see Fig. 9b).

Fig.9: Narrowing of Plasma Centerpost by external vertical field coils

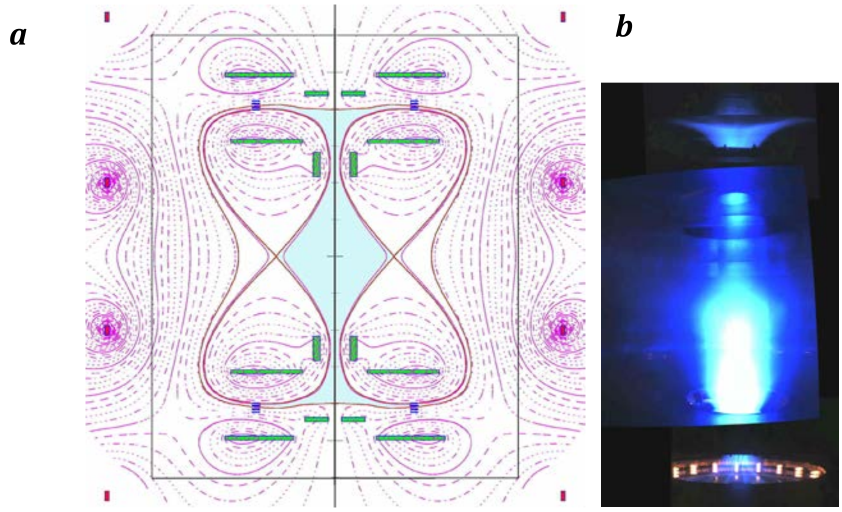

a, Calculated equilibrium of the Plasma Centerpost in absence of any torus, but with the PFExt compression coils added in outside the vessel. b, Centerpost discharge #1098 in Ar at I_e =3 kA: no Torus formation.

However, when the current exceeded ~I_e =8.5 kA in Argon and the rotational transform of the Plasma Centerpost (calculated from anode to cathode) overcame the semi-integer value $\iota_e \geq 1/2$($q_e \leq 2$in terms of the inversely defined safety factor) the Ar Plasma Centerpost took in the equatorial region the approximately spherical shape associated with the torus formation (Fig. 10a): it bulged axisymmetrically much more than in all cases so far shown and exhibited the presence of an axisymmetric double null (DN) divertor. This behavior is exactly what an equilibrium calculation[19] predicts (Fig. 10b) if an axisymmetric torus is formed. Although there are not magnetic measurements near the torus (in Phase-1 no magnetic probes were integrated in the main chamber between the two PF2 "mirror coils", as the formation of a torus was not foreseen) the fit of the distance between the two X-points of the DN divertor is a quite accurate estimate of the current flowing inside the torus: an equilibrium fit of this critical parameter[19] gives for the Argon torus a current I_{ST}= 5 kA (Fig. 10c).

Fig.10: The Argon Tori obtained in Phase-1.

a *b* *c*

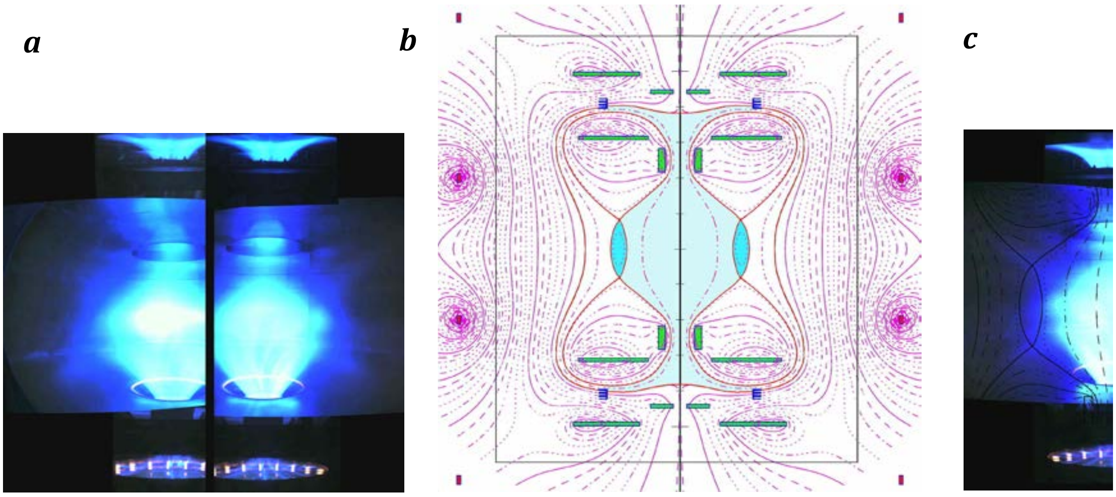

a, Torus in Ar discharge #1149 and #1160 at I_e=10 kA; in the two discharges the fast camera looks at the two opposing sides to show the overall separatrix. b, Calculated equilibrium of a plasma torus carrying a toroidal current I_{ST}=5 kA. c, Torus of Ar discharge #1160 at I_e=10 kA, superposed with the calculated equilibrium at I_{ST}=5 kA.

The Argon tori can be sustained for all the time duration for which the DC voltage is applied between the electrodes that drive the Plasma Centerpost, that is 0.5 sec, because the achievement of steady state conditions for the combined (internal + external) shaping field imposes to wait 0.6 s before the plasma break-down, in order to allow for the skin current in the 4 cm thick Aluminum vacuum vessel to decay. The obtained tori, having an aspect ratio A=7.5 together with an elongation b/a=κ=3.5, have so far never been produced in a Tokamak: with such a high aspect ratio and elongation[20], in particular in absence of a close-fitting conducting wall, a Tokamak discharge would not be sustainable[21,22] and would simply disrupt with a vertical displacement event in a few Alfven times. The most surprising asset is however the unexpected production of a torus from the Plasma Centerpost in absence of any magnetic flux variation, i.e. in a totally magnetostatic configuration of the axisymmetric poloidal magnetic field. The price that has to be payed in term of input power for the formation and for the sustainment of the 5 kA Ar tori is that the break-down voltage increases from 90 V (in absence of the torus) to 200 V, but the voltage at the current flat top increases only from 200 V (in absence of torus) to 220 V. Then the power that the Ar torus sustainment requires is just an additional 200 kW, with respect to the 2.0 MW required by the Ar Plasma Centerpost.

The Hydrogen tori obtained in Phase-1

After the formation of the Argon tori the same endeavor was successfully attempted with a Hydrogen plasma. The presence of Hydrogen tori is most evident when the plasma begins (Fig. 11) and when it terminates (Fig. 12).

The confined torus appears since the first milliseconds after the plasma break-down (the Plasma Centerpost current I_e reaches its flat top value in ~6 msec) and disappears at a slower rate than the unconfined Plasma Centerpost, which decays in ~3 msec.

Fig.11: Hydrogen torus 5 msec after plasma break-down.

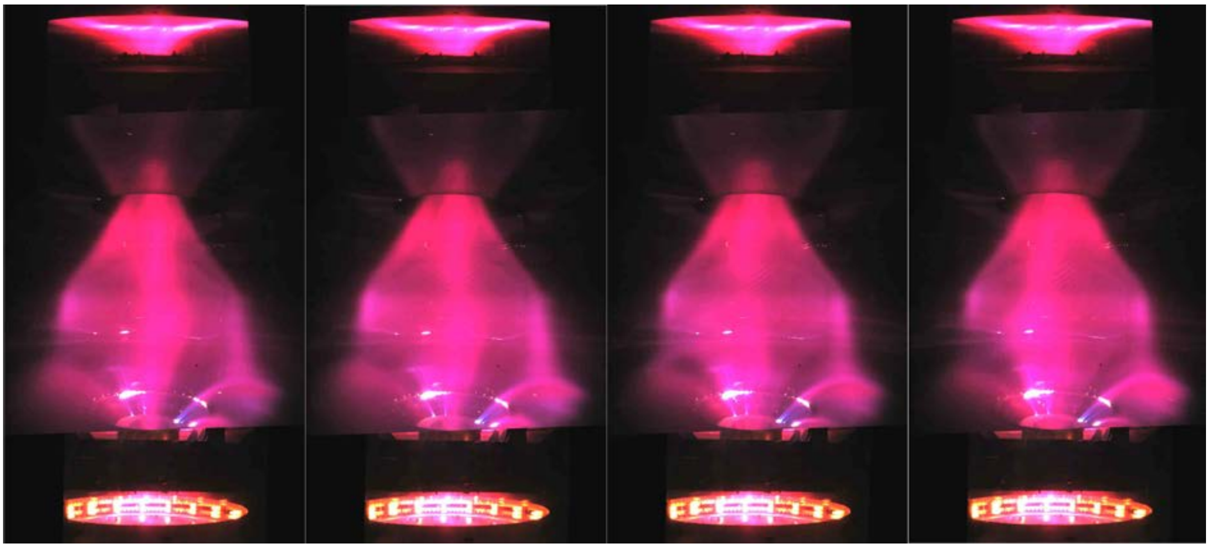

Frame sequence of torus formation in H discharge #1202, starting from 5 ms after plasma break-down (the Plasma Centerpost current reaches I_e=10 kA in 6 ms), all these frames of the equatorial fast camera (1/3 ms time resolution) are separated by 1 ms, but the images of the two anode and cathode slow cameras are always the same (11 ms time resolution).

Fig.12: Hydrogen torus during the last 3 msec of plasma discharge.

a

b

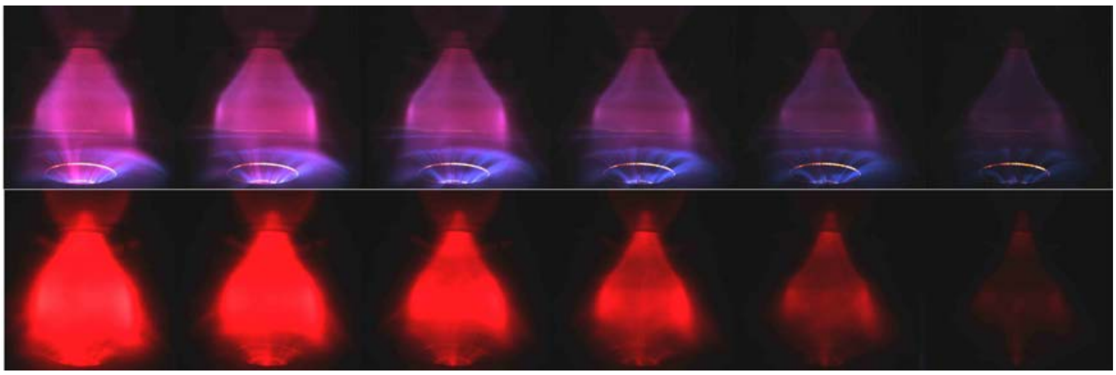

a, Top: Sequence of visible light images, during termination of H discharge #1224 which ramps down from I_e=10 kA in 3 ms; all these frames of the equatorial fast camera are separated by 1/3 ms. b, Bottom: same for H discharge #1219, observed through a H-alpha interferometric filter.

Fig. 13 evidences that in the last ms of the discharge even the confined current flowing inside the Torus persists for much longer than the unconfined current flowing between electrodes: as a matter of fact near the termination of the Plasma Centerpost current decay the torus becomes kink unstable, indicating that the ratio of its poloidal field (due to its toroidal confined current) with respect to its toroidal field (due to the Centerpost unconfined current) becomes too large.

Fig.13: Hydrogen Torus kinking during last 1 msec of plasma discharge.

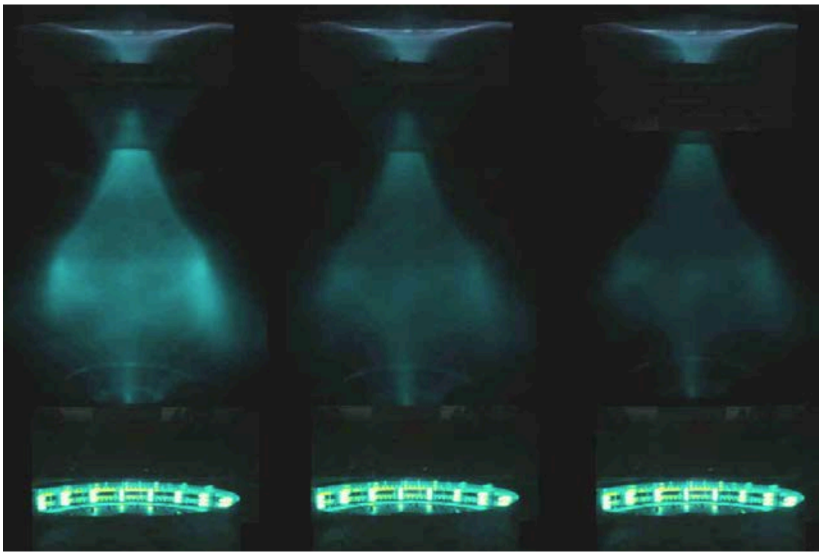

Terminal sequence of plasma (last ms), observed through H-alpha interferometric filter, but rendered by cold-warm color involution, H discharge #1219; frames separated by 1/3 ms.

The tori are limited by a magnetic separatrix endowed with 2 conical divertor fans. Already in Ar the lower (cathodic) divertor fan is often dominant (see Fig. 10a), but the H torus has a very bright ant totally dominant cathodic (lower) fan: in order to cure this problem a new lower divertor metal plate is being inserted inside the machine.

The H tori were sustained for only 0.25 sec (see Fig. 14), just because of the excessive interaction of the lower divertor fan (see Fig. 15) with the inappropriate lower polycarbonate diaphragm, which, when built, was not deemed to be used as a divertor plate.

Fig.14: H torus sustained for ¼ of sec.

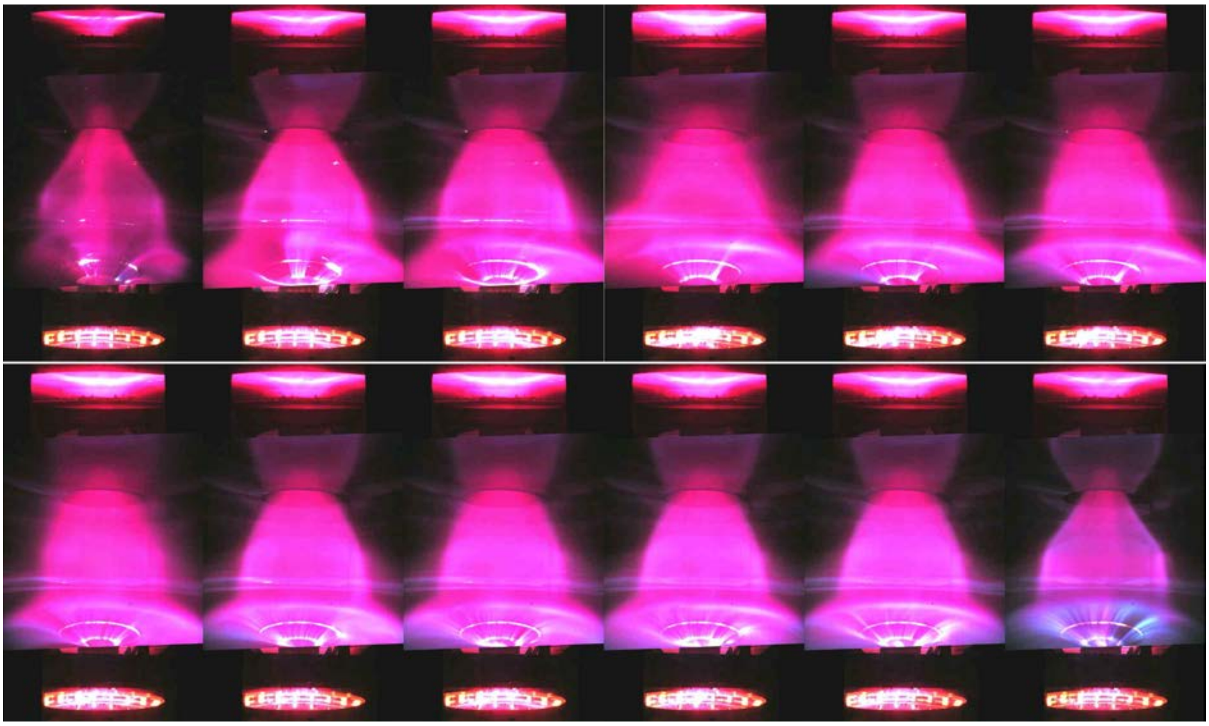

Frame sequence of equally time-spaced, visible light pictures of Torus sustainment in H discharge #1202, lasting 0.25 sec, with I_e=10 kA. The translucent polycarbonate lower diaphragm and the thin cylindrical lining disturb the images by reflecting the bright lower divertor fan.

Furthermore the troublesome lower (cathodic) divertor fan causes spurious paths of the plasma current: from the lower divertor fan, to the evaporating lower diaphragm and finally to the cathode, lapping against the polycarbonate. The robustness of the Plasma Centerpost+Torus configuration of PROTO-SPHERA is however apparent as the Tori have not disrupted: they have just survived, albeit vertically displaced, even in presence of these wrong current paths in the lower part of the Plasma Centerpost, which greatly modify the overall plasma equilibrium.

Fig.15: H torus lower divertor fan with an inappropriate divertor plate.

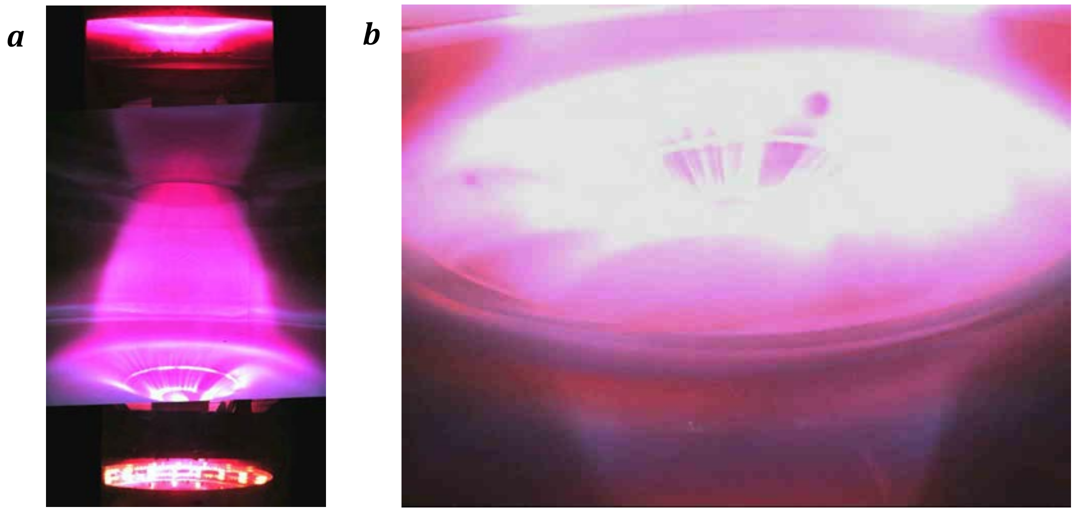

a, Divertor fan interacting with the lower polycarbonate diaphragm in H discharge #1202. b, Same observed by a tilted camera looking at the whole diaphragm

The H tori obtained is so far have an aspect ratio A~7 and an elongation b/a=κ~3.5, in rough agreement with equilibrium calculation of Fig. 8b, in which the torus carries I_{ST}=7 kA. The vertical field required by Argon Tori, in terms of the current flowing in the PFext coils (fed in series with the Group-B PFInt coils), was 12.5% smaller than the maximum current that the PFInt power supply could deliver. Instead for Hydrogen tori the vertical field current requirement turned out to be 25% larger than the maximum current that the PFInt power supply could deliver to both Group-B PFInt coils in series with the PFExt additional coils. The missing PFExt current required by H tori was matched by feeding a few turns of the two PFExt nearer to the equator with a further new power supply based upon Supercapacitors[23] (2 kA at 96 V DC for a few sec, with a rise time longer than 20 ms). Also the ratio 1.25/0.875 ~1.43, between the vertical field that Hydrogen tori require with respect the vertical field that is sufficient for Argon tori, confirms that the ratio of toroidal currents confined inside the tori is I_{ST} ~7 kA in H, with respect to I_{ST} ~5 kA in Ar. The price that has to payed in term of input power for the ~7 kA H tori is that the break-down voltage increases only from 320 V (in absence of torus) to 360 V (even slightly beyond the nominal maximum value of the Plasma Centerpost power supply), but the voltage at the current flat top increases from 220 V (in absence of torus) to 320 V. Then the additional power that the H tori require is about 1 MW, with respect to the 2.2MW required by the H Plasma Centerpost. However it has to be remarked that this large power is not the power required for the sustainment of H tori, but is presumably due to the inappropriate interaction with the lower polycarbonate diaphragm and to the wrong current paths in the lower part of the Plasma Centerpost.

If the vertical field is in slight eccess with respect to the optimum value, say 10%, the Plasma Centerpost produces odd configurations like Double Tori (Fig. 16a) and lop-sided Tori (Fig. 16b), all with visible helical components. However the Plasma Centerpost and the Tori never disappear: in the PROTO-SPHERA configuration there isn't any event similar to the disruptions that plague the Tokamak configuration. Instead there are cases in which, after a reduced current plasma start-up where I_e remains below 5 kA for quite long times (even up to 0.15 sec), the Plasma Centerpost finally achieves 10 kA and forms a proper single torus around the Plasma Centerpost; the torus is thereafter sustained until the the DC voltage is applied to the electrodes.

Fig.16: Vertical field in excess: double tori and lop-sided tori.

a ***b***

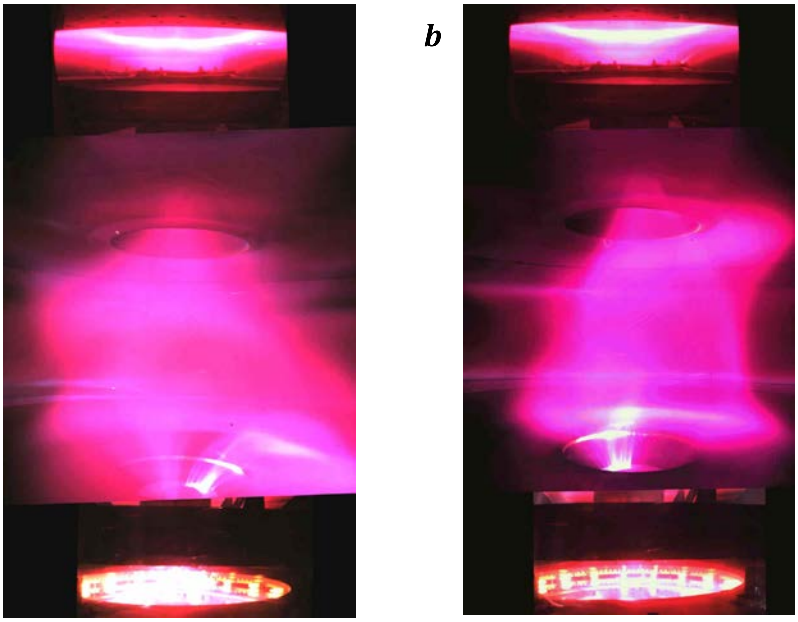

a, The vertical field is in slight eccess for H discharge #1211 (with I_e=10 kA) and produces double Tori, with some helical component. b, The vertical field is also in eccess for H discharge #1225 and produces lop-sided double Tori, with large helical components.

Fig. 17 illustrates the evolution of shot #1219, with total duration of 250 ms, where the Plasma Centerpost current remains below 5 kA for ~70 ms (first 4 time slices) in a sort of star-shaped plasma, and later increases to 8 kA with a double Torus configuration evolving only in the last 100 ms to a proper Torus around the Plasma Centerpost.

Fig.17: The metamorphosis of an axisymmetric toroidal cusp into a torus.

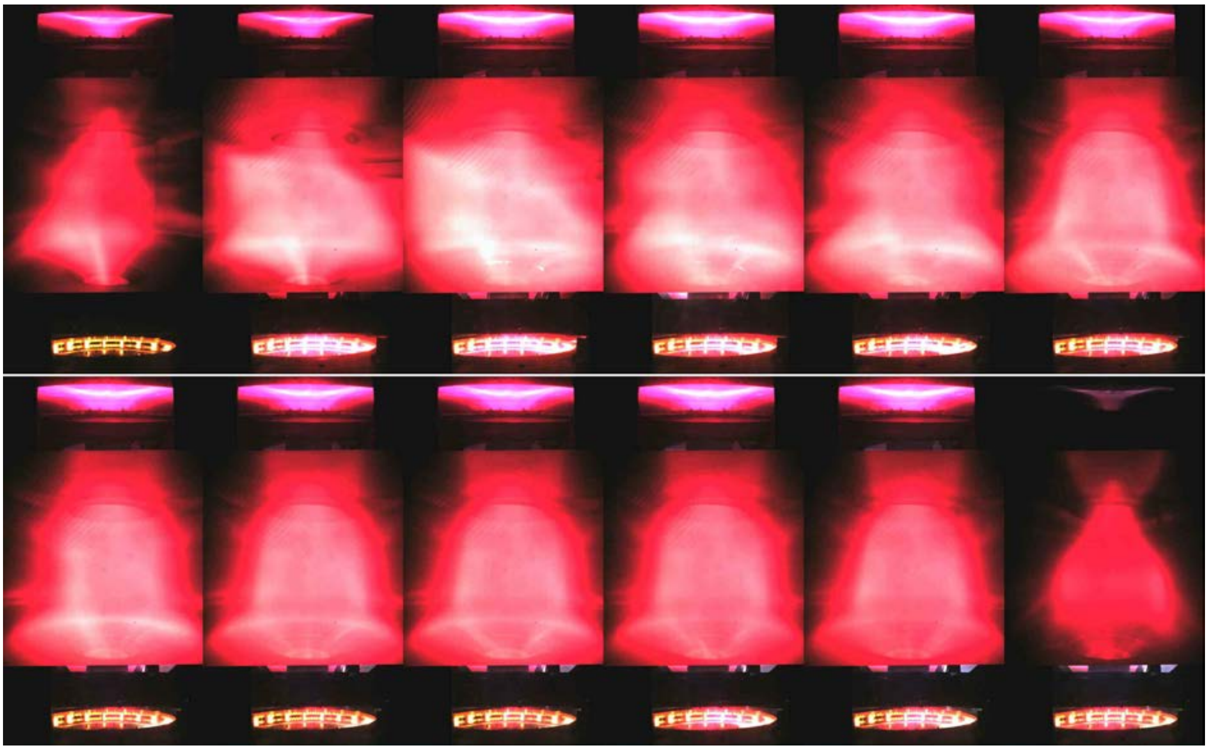

Frame sequence (left to right, top to bottom) of equally time-spaced (H-alpha filtered) images of the H discharge #1219, lasting 0.25 sec. The first 3 frames are characterized by the Centerpost plasma current not being able to overcome I_e=5 kA and by the absence of the Torus, later I_e reaches 10 kA and the configuration metamorphoses into a torus.

This initial difficulty in Hydrogen plasma to form a torus, when the Plasma Centerpost current I_e is insufficient, is similar to what occurs in Argon plasma (see Fig. 9b); the plasma discharge has a part where the current flows in the Plasma Centerpost but the rest of the plasma discharge seems trapped in a axisymmetric toroidal cusp configuration[24,25] (Fig. 18a, 18b), however the larger power input to the clamped current plasma (1.5 MW in H vs. 360 kW in Ar) allows for a much larger light emission, which indicates more clearly the hexapolar character of the poloidal field pre-existent to the plasma (Fig. 18c).

Also the required poloidal field for PROTO-SPHERA in Phase-2, able to shape and compress the largest current in the torus (I_{ST}=240 kA), has a mainly hexapolar character, with the complication that the two electrodes become disconnected from each other, in terms of the pre-imposed axisymmetric configuration of static poloidal field (see Fig.18d); this disconnection implies possible difficulties in setting up a proper Plasma Centerpost in a purely static poloidal field pre-existent to the plasma.

Fig.18: Poloidal fields pre-existent to plasma are axisymmetric cusps.

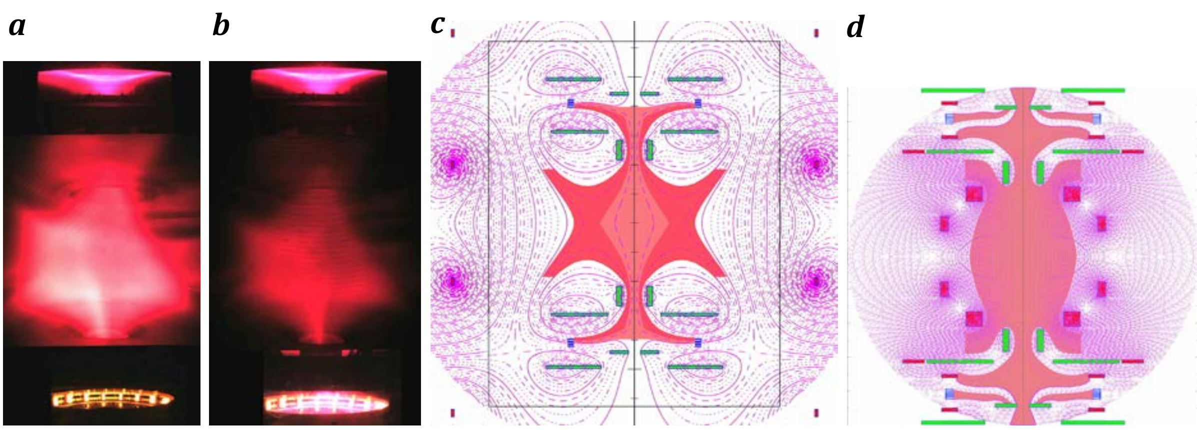

a, The plasma discharge has a low current Plasma Centerpost, but is as well trapped in a axisymmetric hexapolar toroidal cusp configuration, in the initial H shot #1219. b, Same for the initial H shot #1221. c, The hexapolar character of the poloidal field pre-existent to the plasma break-down in those two shots. d, The hexapolar character of the poloidal field pre-existent to the ¼ MA Spherical Torus of PROTO-SPHERA in Phase-2: the two electrodes become disconnected from each other, in terms of the pre-existing axisymmetric configuration of static poloidal field.

Therefore it seems possible that PROTO-SPHERA in Phase-2 could not be able to form a confined Spherical Torus in perfectly steady poloidal magnetic field, but that the torus will be formed increasing, on a time scale of a few tens of msec, both the Plasma Centerpost current I_e to 60 kA, along with the current in the Group-A PFInt compression coils; such a slow rise time opens the possibility of a feedback vertical field controlled formation of the Spherical Torus and dispels the original and risky idea[8] that a very fast formation (~1 msec) could be required for producing the torus in Phase-2.

A new insulating vacuum vessel (made out of very thick transparent PMMA, poly-methyl-methacrylate) will be installed in 2019, then the problem of the skin current inside the present Aluminum vessel will disappear; four new PFExt external field coils with less resistance will be set up as well around the PMMA vessel, such that the existing Supercapacitor power supply will be able to feed the whole new PFExt series of coils; it will therefore become possible to test already in Phase-1 an impulsive torus formation with a 20 ms rise time.

Magnetic reconnections as origin and sustainment of the torus in PROTO-SPHERA

The clear evidence that the Hydrogen plasma forms a torus since the first milliseconds after the plasma break-down in perfectly static field conditions rules out any possible interpretation in terms of inductive phenomena: the only induction could be the one associated with the current increase in the Plasma Centerpost itself, just after the break-down, which would imply a loop voltage of less than 0.1 V for a few ms only and moreover in the direction opposite to the direction of the current that flows around the Plasma Centerpost: such a short duration opposite current in the torus could not be held in equilibrium by the external vertical field applied by the PFExt coils. The field imposed by the PFInt coils is going upwards near the symmetry axis of the machine, whereas the current density is going downwards from the upper anode to the lower cathode, so in the Plasma Centerpost the sign of $\vec{j} \bullet \vec{B}$ is negative and the plasma current winds in the Centerpost in the anticlockwise direction, as seen from above. Also the current in the torus is anticlockwise, as the current in the PFExt coils has been setup in the clockwise direction (both always seen from above). Then the sign of the toroidal current in the torus is the same as the sign of the toroidal current in the Plasma Centerpost and also the sign of $\vec{j} \bullet \vec{B}$ is negative all over the plasma, both in the centerpost as well as in the torus[26,27]. This is a clear sign that the current in the torus is due to DC Helicity Injection from the Centerpost to the torus, just as it was imagined when the PROTO-SPHERA experiment was designed. That magnetic reconnections are responsible for the production and for the sustainment of the torus comes from the presence of ordinary X-points in the DN divertor (in Hydrogen almost always replaced by a SN divertor): magnetic reconnection in the two dimensional approximation occur naturally at ordinary X points[28], albeit 3D effects[29] are certainly present, as indicated from the somewhat diffused (ergodic) character of the X-points observed in PROTO-SPHERA.

The second hint to magnetic reconnection is, in the case of Hydrogen tori, the repetition of distinctive bursts that shake the shape and the extent of the plasma, with irregular quasi-periodicity, but usually separated by 2-3 msec:

all such events are accompanied by emissions of plasma into the separatrix fans.

Fig.19: Repetitive burst of plasma extent during magnetic reconnections.

a ***b***

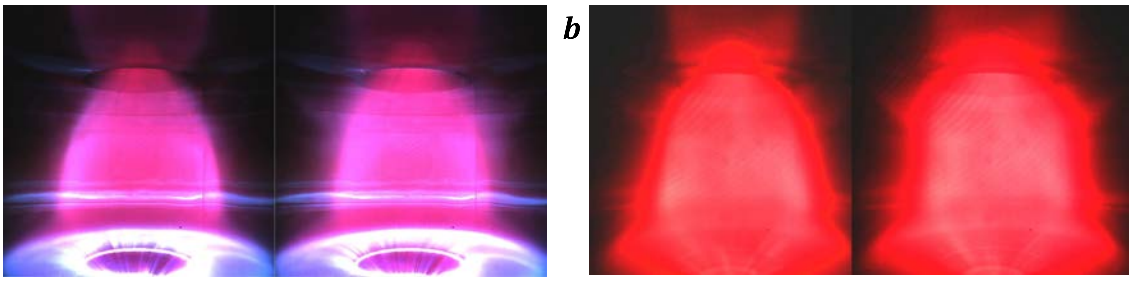

a, Typical excursion of the plasma extent, observed in visible light, associated with a magnetic reconnection, in H shot #1195. b, Same for shot #1219, through an H-alpha filter.

These occurrences are quite reminiscent of the bursting nature of the "Flux Transfer Events" in the Earth Magnetosphere[30] and of "Solar Flare X-Ray Emission" [31], not to mention the repetitive, but not fully periodic, occurrence of "Sawtooth Oscillatins" [32,33] and of "ELM's activity" [34,35] in Tokamaks. An example of the excursions in the shape and extent of plasma images are shown in Fig.19a in visible light and in Fig. 19b in H-alpha filtered light. In Argon tori the separatrix fan is less extended and the emission of plasma into the fans is more continuous.

Conclusions

The main results illustrated in this paper deal with the first production of plasma tori in the PROTO-SPHERA experiment, they indicate that:

1) There is no unavoidable need of a toroidal magnet for producing quasi-axisymmetric magnetically confined tori: a Plasma Centerpost discharge, sustained by DC voltage between two electrodes, is sufficient for obtaining such an aim.
2) The tori are produced in a pre-existing axisymmetric configuration of magnetostatic poloidal field (which is, in the present Phase-1 of the PROTO-SPHERA experiment, mainly a vertical field): no variations are required in the poloidal fields that (as per the virial theorem) surround and contain the plasma.
3) The magnetically confined tori can be sustained in quasi-steady state, i.e. for all the time duration for which the DC voltage is applied between the electrodes that sustain the Plasma Centerpost. The explanation that the authors offer for such behavior is that magnetic reconnections associated with the divertor configuration of the machine are able to provide a completely steady-state current drive to the toroidal plasma. After many decades during which magnetic reconnections were the nightmare of many magnetic containment schemes, the first useful application of these basic plasma phenomena could have appeared in magnetic confinement, hopefully to be consolidated by more significant plasma discharges in future

experiments, if possible to be further extended to obtain plasma heating[36,37,38] and maybe to remain finally as a useful tool in magnetic Controlled Fusion research.

4) No disruption phenomena occur in the PROTO-SPHERA magnetic confinement configuration, up to now at most multiple tori or lop-sided tori, with relevant non-axisymmetric components, were obtained if the applied vertical field is beyond its "proper value". Similarly even wrong current paths in the lower part of the Plasma Centerpost, like the ones obtained from the lower divertor plate (which happened by chance to be also built from a completely inadequate material) to the cathode, are not able to disrupt the tori, which become simply vertically displaced.
5) The resilience of the Plasma Centerpost + Torus configuration so far obtained is up to now greater than the resilience of the Tokamak configuration, not only from the point of view of absence of disruptions illustrated in the previous point, but also for its ability to produce tori (like the first ones here illustrated that have an aspect ratio A=7 and an elongation κ=3.5), that in a Tokamak could absolutely not be produced and sustained.

All these points, when put together, give an even stronger conclusion: magnetic confinement devices to study Controlled Fusion could in principle be built using axisymmetric permanent magnets only, able to provide a poloidal magnetostatic field pre-existent to the plasma. A Plasma Centerpost fed by electrodes will produce and sustain the confined torus in such a poloidal field. In case the two electrodes become disconnected from each other, in terms of the pre-imposed axisymmetric configuration of permanent magnet poloidal field (see Fig. 18d for PROTO-SPHERA Phase-2), the help of short duration currents, from a few simply conducting coils, would be required in addition to the permanent magnets: however the currents of these simply conducting coils could be gradually switched off during the start-up of the plasma and would vanish when the proper final confinement configuration, to be sustained by permanent magnets only, is achieved.

References

1 M. Tuszewski, Field Reversed Configurations, *Nucl. Fusion* **28**, 2033 (1988)

2 F. Rogier, G. Bracco, A. Mancuso, P. Micozzi, and F.Alladio, Simply Connected High-Beta Magnetic Configurations, *11TH INTERNATIONAL CONGRESS ON PLASMA PHYSICS: ICPP 2002, AIP Conference Proceedings* **669**, 557 (2003)

3 J. Wesson, *Tokamaks, 4th ed.*, Oxford University Press, Oxford (2011)

4 D.H. Crandall, , C.W. Hartman, Y.K.M. Peng, A.L. Hoffman, R.A. Krakowski, J.D. Sethian, A.E. Robson, Reversed field pinch, Compact Toroids, and Dense Z-pinch, *J Fusion Energy* **8**, 9–25 (1989)

5 J. Manickam, Allen H. Boozer, and Stefan Gerhardt, Kink modes and surface currents associated with vertical displacement events, *Phys. Plasmas* **19**, 082103 (2012)

6 Allen H. Boozer, What is a stellarator?, *Physics of Plasmas* **5**, 1647 (1998)

7 F. Alladio, A. Mancuso, P. Micozzi, L. Pieroni, C. Alessandrini, G. Apruzzese, L. Bettinali, P. Buratti, A. Coletti, P. Costa, C. Crescenzi, A. Cucchiaro, R. De Angelis, T. Fortunato, D. Frigione, M. Gasparotto, G. Gatti, R. Giovagnoli, L.A. Grosso, G. Maddaluno, G. Maffia, S. Mantovani,

G. Monari, C. Nardi, S. Papastergiou, M. Pillon, A. Pizzuto, M. Roccella, F. Rogier, M. Santinelli, L. Semeraro, A. Sibio, B. Tilia, O. Tudisco, L. Zannelli, V. Zanza, PROTO-SPHERA, ENEA, Serie Energia, Associazione Euratom-ENEA sulla Fusione, RT/ERG/FUS/2001/14, ISSN: 1124-7932 (2001)

8 F. Alladio, P. Costa, A. Mancuso, P. Micozzi, S. Papastergiou and F. Rogier, Design of the PROTO-SPHERA experiment and of its first step (MULTI-PINCH), *Nucl. Fusion* **46**, S613–S624 (2006)

9 Alessandro Lampasi, Giuseppe Maffia, Franco Alladio, Luca Boncagni, Federica Causa, Edmondo Giovannozzi, Luigi Andrea Grosso, Alessandro Mancuso, Paolo Micozzi, Valerio Piergotti, Giuliano Rocchi, Alessandro Sibio, Benedetto Tilia and Vincenzo Zanza, Progress of the Plasma Centerpost for the PROTO-SPHERA Spherical Tokamak, *Energies* **9**(7), 508 (2016)

10 A. Sykes, E. Del Bosco, R.J. Colchin, G. Cunningham, R. Duck, T. Edlington, D.H.J. Goodall, M.P. Gryaznevich, J. Holt, J. Hugill, J. Li, S.J. Manhood, B.J. Parham, D.C. Robinson, T.N. Todd and M.F. Turner, First results from the START experiment, *Nucl. Fusion* **32**, 694 (1992)

11 F. Alladio, L.A. Grosso, A. Mancuso, S. Mantovani, P. Micozzi, G. Apruzzese, L. Bettinali, P. Buratti, R. De Angelis, G. Gatti, G. Monari, M. Pillon, A. Sibio, B. Tilia, O. Tudisco, Results of Proto-Pinch Testbench for the Proto-Sphera experiment, *Proc. of the 27th EPS Conference on*

Contr. Fusion and Plasma Phys. Budapest, 12-16 *June* 2000, ECA Vol. 24B, 161-164 (2000)

12 O. Tudisco, A. Lucca Fabris, C. Falcetta, L. Accatino, R. De Angelis, M. Manente, F. Ferri, M. Florean, C. Neri, C. Mazzotta, D. Pavarin, F. Pollastrone, G. Rocchi, A. Selmo, L. Tasinato, F. Trezzolani, and A. A. Tuccillo, A microwave interferometer for small and tenuous plasma density measurements, *Review of Scientific Instruments* **84**, 033505 (2013)

13 F. Brandi, F. Giammanco, W. S. Harris, T. Roche, E. Trask, and F. J. Wessel, Electron density measurements of a field-reversed configuration plasma using a novel compact ultrastable second-harmonic interferometer, *Review of Scientific Instruments* **80**, 113501 (2009)

14 T. Del Rosso, F. Giammanco, M. G. Anderson, F. Conti, A. Balvis, I. Isakov, V. Matvienko, G. Strashnoy, W. Waggoner, L. Bonelli, E. Paganini, and M. W. Binderbauer, Long-path second-harmonic interferometer with nanosecond time resolution: reliable diagnostic tool for electron density measurement in pulsed plasma devices, *Optics Letters* **37**, No. 18 3855 (2011)

15 V. Lazic, A. De Ninno, Calibration approach for extremely variable laser induced plasmas and a strategy to reduce the matrix effect in general, *Spectrochimica Acta Part B* **137**, 28–38 (2017)

16 H. A. Bethe and C. L. Critchfield, The formation of Deuterons by Proton combination, *Phys. Rev.* **54**, 248 (1938)

17 D.L. Murphree, R.P. Carter, Observations on magnetically induced anodic arc region behavior, *Journal of Applied Physics* **45**, 1915 (1974)

18 H.C. Miller, A review of anode phenomena in vacuum arces, *Contributions to Plasma Physics* **23**, 223-249 (1989)

19 F.Alladio and P. Micozzi, Reconstruction of Spherical Torus Equilibria in Absence of Magnetic Measurements in the Central Cavity, *Nucl. Fusion* **37**, 1759 (1997)

20 S. C. Cowley , P. K. Kaw , R. S. Kelly , and R. M. Kulsrud, An analytic solution of high beta equilibrium in a large aspect ratio tokamak, *Physics of Fluids* B **3** , 2066 (1991)

21 R.D. Stambaugh, L.L. Lao, E.A. Lazarus, Relation of vertical stability and aspect ratio in Tokamaks, *Nucl. Fusion* **32**, 1642-1646 (1992)

22 R. Fitzpatrick, A sharp boundary model for the vertical and kink stability of large aspect-ratio vertically elongated tokamak plasmas, *Physics of Plasmas* **15**, 092502 (2008);

23 G. Maffia, A. Lampasi, and P. Zito, A new generation of pulsed power supplies for experimental physics based on supercapacitors, *IEEE 15th*

International Conference on Environment and Electrical Engineering (EEEIC), 1067-1072 (2015)

24 J.B. Taylor, Some Stable Plasma Equilibria in Combined Mirror-Cusp Fields, *Physics of Fluids* **6**, 1529 (1963)

25 R. Jones, Plasma confinement in an axisymmetric toroidal multipole cusp, *Il Nuovo Cimento B* **78**, pp 249–254 (1983)

26 J.B. Taylor, *Phys. Rev. Lett.* **33**, 1139 (1974)

27 J.B. Taylor and M.F. Turner, Plasma current drive by helicity injection in relaxed states, *Nucl. Fusion* **29**, 219-229 (1989)

28 R.L. Stenzel and W. Gekelman, Magnetic Field Line Reconnection Experiments 1. Field Topologies, *Journal of Geophysical Research* **86**, 649-658, (1981)

29 V.E. Parnell, J.M. Smith, T. Neukirch, and E.R. Priest, The structure of three-dimensional magnetic neutral points, *Phys. Plasmas* **3**, 759-770 (1996)

30 D. J. Southwood, C. J. Farrijgia And M. A. Saunders, What Are Flux Transfer Events?, *Planet. Space Sci.* **36**, 505-508, (1988)

31 P. E. Fehlau, W. H. Chambers, J. C. Fuller, W. E. Kunz, R. W. Milkey And N. K. Blocker, Periodic Solar Flare X-ray Emission, *Nature* **232**, 42–43 (1971)

32 V. Goeler, et al. Studies of internal disruptions and m= 1 oscillations in tokamak discharges with soft−x-ray techniques, *Phys. Rev. Lett.* **20**, 1201 (1974)

33 BB. Kadomtsev, Disruptive instability in tokamaks, *Soviet Journal of Plasma Physics* **1**, 389-391 (1975)

34 F. Wagner, G. Becker, K. Behringer, D. Campbell, A. Eberhagen, W. Engelhardt, G. Fussmann, 0. Gehre, J. Gernhardt, G.V. Gierke, G. Haas, M. Huang, F. Karger, M. Keilhacker, Q. Kluber, M. Kornherr, K. Lackner, G. Lisitano, G.G. Lister, H.M. Mayer, D. Meisel, E.R. Müller, H. Murmann, H. Niedermeyer, W. Poschenrieder, H. Rapp, H. Bohr, F. Schneider, G. Siller, E. Speth, A. Staebler, K.H. Steuer, G. Venus, O. Vollmer, and Z. Yu., Regime of Imyroved Confinement and High Beta in Neutral-Beam-Heated Divertor Discharges of the ASDEX Tokamak, *Phys. Rev. Lett.* **49**, 1408-1412 (1982)

35 A. Kirk, H.R. Wilson, R. Akers, N.J. Conway, G.F. Counsell, S.C. Cowley, J. Dowling, B. Dudson, A. Field, F. Lott, B. Lloyd, R. Martin, H. Meyer, M. Price, D. Taylor, M. Walsh and the MAST team, Structure of ELMs in MAST and the implications for energy deposition, *Plasma Phys. Control. Fusion* **47**, 315 (2005)

36 R.L. Stenzel, W. Gekelman, and N. Wild, Magnetic Field Line Reconnection Experiments 4. Resistivity, Heating, and Energy Flow, *Journal of Geophysical Research* **87**, 111-117 (1982)

37 E.G. Zweibel and Masaaki Yamada, Magnetic Reconnection in Astrophysical and Laboratory Plasmas, *Annu. Rev. Astron. Astrophys.* **47**, 291–332 (2009)

38 E.G. Zweibel and M. Yamada, Perspectives on magnetic reconnection, *Proc. R. Soc. A* **472**, 20160479 (2016)